DIRECT NUMERICAL SIMULATION OF A TRANSITIONAL RECTANGULAR JET

B. Rembold, N. A. Adams and L. Kleiser
Institute of Fluid Dynamics, ETH Zürich,
ETH Zentrum, CH-8092 Zürich, Switzerland
rembold@ifd.mavt.ethz.ch

ABSTRACT

A highly accurate numerical study of a Mach 0.5 jet exiting from a rectangular shaped nozzle with an aspect ratio of 5 into a quiescent ambient was performed at a Reynolds number of 2000 based on the narrow side of the nozzle. The transition process was triggered using the most unstable symmetric linear eigenmode of a parallel laminar jet profile for excitation at the inflow. We observe a shear-layer roll-up of the laminar jet and a very rapid transition to small scale turbulence. The non-axisymmetry of the velocity profile downstream of the nozzle leads to a rapid spreading of the jet along its minor axis in the characteristic region as is expected from experiments.

1. INTRODUCTION

Due to their significance in practical applications (propulsion, combustion) jet flows have been extensively studied in the past, experimentally as well as numerically. Recently, non-axisymmetric jet configurations found increased attention owing to their superior mixing properties compared with round jets (Gutmark and Grinstein, 1999). Computational studies of these flows are being performed in order to identify means to increase mixing, accelerate break-up, or reduce radiated noise. Most Direct Numerical Simulations (DNS) and Large-Eddy Simulations (LES) have been performed for round or planar jets. Much less computational and experimental data exist for fully three-dimensional nozzle shapes. In this study, a high-order simulation method has been developed for non-axisymmetric jet flows solving the three-dimensional compressible Navier-Stokes equations on a Cartesian domain. The main objectives of this study are (i) to investigate in detail the dynamics of rectangular jets at a sufficiently low Reynolds number at which DNS is feasible, and (ii) to provide reference data for later validation of LES. We point out that a direct comparison of LES results with experiments is problematic since the experimental inflow conditions are affected by nozzle and reservoir geometries and can be matched only approximately in the simulations.

2. FLOW CONFIGURATION

A rectangular jet configuration was chosen with an aspect ratio of $L_1/L_2 = 5$, a Reynolds number based on the jet center velocity and the height of the nozzle exit L_2 of 2000 and a Mach number of 0.5. The configuration and the coordinate system is illustrated in figure 1. We denote the $y-$axis as the major and the $z-$axis as the minor jet axis, respectively. The geometry and flow parameters except for the Reynolds number were chosen as to match the experiments of Tsuchiya *et al.* (1986). The computational domain measures $37.5L_2 \times 35L_2 \times 35L_2$ (x, y, z). This is large enough to capture the beginning of the *characteristic-decay* region of the mean velocity at the jet center as defined by Sforza and Steiger (1966), however, it does not extend into the subsequent *axisymmetric-decay* region.
We do not model the nozzle itself in the domain, but instead use an inflow profile with velocity half widths corresponding to the nozzle dimensions. For the simulations a laminar smoothed top-hat inflow profile for the streamwise velocity component according to Yu and Monkewitz (1990)

$$u(\eta) = \frac{1}{1 + \sinh(|\eta| \cdot \sinh^{-1}(1))^{2n_i}} \qquad (1)$$

was used along the jet centerlines. Here η is the cross-stream coordinate which is normalized with the corresponding velocity half-width $L_i/2$, ($i = 1, 2$). The parameters $n_1 = 9$ and $n_2 = n_1 L_2/L_1$ are chosen to ensure equal vorticity thicknesses $\delta = \delta_i = L_i/(\sqrt{2}\, n_i \sinh^{-1}(1))$ in both directions. The

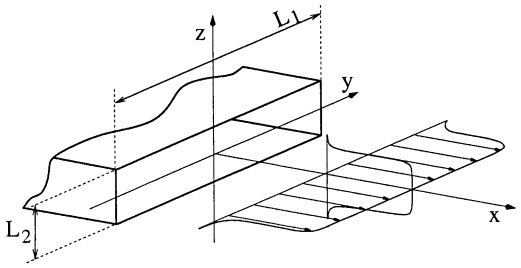

Figure 1: Jet geometry and coordinate system.

cross-stream velocity components of the laminar inflow profile are zero.

3. STABILITY ANALYSIS

The transition process of the jet is very sensitive to minor changes in the inflow condition, that can lead to an excitation of different instability modes in the laminar jet. By merely enforcing a laminar profile as described above transition would be triggered mainly by numerical roundoff errors. It is therefore important to impose clearly defined inflow disturbances. In this simulation we use a spatially developing unstable eigensolution of linear stability theory to initiate transition in a controlled way. Based on the velocity profile (1) and assuming parallel two dimensional flow we performed an inviscid spatial linear stability analysis to compute the most unstable non-oblique spatial modes, which are the sinuous (asymmetric) and varicose (symmetric) mode, respectively. In our simulation we then superimpose the varicose mode of the plane jet profile to the laminar inflow profile (see below, boundary conditions). In figure 2 the eigenfunction of the streamwise velocity component is shown for the spatially most amplified varicose mode.

4. SIMULATION METHOD

Numerical procedure

The three-dimensional compressible Navier-Stokes equations in conservation form are solved on a Cartesian grid. For the spatial discretization a fifth order compact upwind-biased scheme (Adams and Shariff, 1996) is used for the convective terms and a sixth order compact central scheme (Lele, 1992) for the diffusive terms. For time integration a third order low-storage Runge-Kutta scheme (Williamson, 1980) is implemented for all terms. We use a Cartesian grid with $337 \times 229 \times 229$ points in (x, y, z) which is condensed in the jet center area in the cross-stream and equidistant in the downstream direction. The refinement in the cross-stream directions is achieved by a hyperbolic tangent coordinate mapping.

Boundary conditions

For the simulation of turbulent flow in an open environment the formulation of the open space boundary conditions is crucial. On one hand, large vortical structures have to leave the computational domain at the outflow boundary without being unphysically reflected, and on the other hand entrainment has to be allowed in the cross-stream directions. Additionally, acoustic waves originating from the transition region must be allowed to leave the domain without affecting the flow by backward reflection. The accurate and efficient formulation of these open space boundary conditions for fully three-dimensional cases is basically an unsolved problem. However, it is found in practical simulations (e.g. Adams (1998) and Stanley and Sarkar (1999)) that a combination of one-dimensional non-reflecting boundary conditions (Thompson, 1987) and sponge layers, which are added at the far field boundaries, leads to reasonable results. In the sponge layers the governing transport equation for the vector of conservative variables $\mathbf{U}$ is modified according to

$$\frac{\partial \mathbf{U}}{\partial t} = \mathbf{F}(\mathbf{U}) - \sigma(\mathbf{U} - \mathbf{U}_0) \quad , \qquad (2)$$

where we have written the spatial Navier-Stokes operator briefly as $\mathbf{F}(\mathbf{U})$, so that the solution is driven towards a given steady mean solution $\mathbf{U}_0$. The coefficient $\sigma = \sigma(x)$ is non-zero only in the sponge layers and is of the form

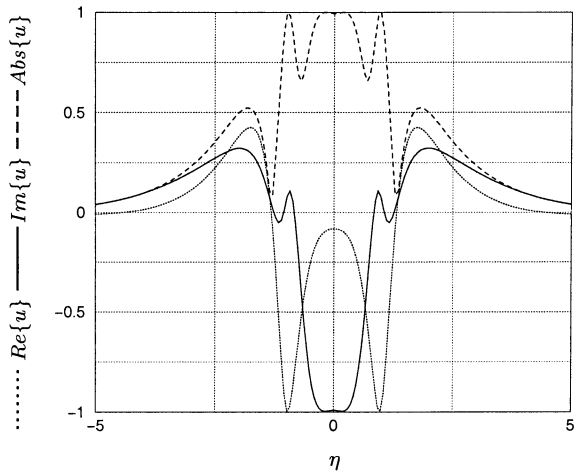

Figure 2: Eigenfunction of the streamwise velocity component across the jet profile coordinate.

$\sigma(\xi) = \alpha\ \xi^{\beta}$, $0 < \xi < 1$, where ξ denotes a normalized coordinate across the sponge. This numerical algorithm was validated by comparison with linear stability theory. Growth-rate comparisons for unstable eigensolutions of parallel jets have shown a very good agreement with linear theory, where for σ the parameters $\alpha = 2, \beta = 3$ were used. The sensitivity of the results to the sponge parameters α and β is weak.

In this simulation the mean solution $\mathbf{U}_0$ is chosen to be equal to the quiescent ambient flow, except at the outflow, where a two-dimensional Gaussian velocity profile is prescribed with velocity half widths estimated from experimental data. The mass flux through the outflow is matched to the influx through the jet. At the inflow plane we apply Dirichlet conditions and use an additional sponge layer outside of the jet inflow region to prevent spurious reflections from the inflow boundary. The inflow mean profile is chosen according to Eqn. (1) along the two axes of the jet profile. Along the center of the rectangular inflow profile ($|y| < L_1/2$) we assume the flow to be mainly two-dimensional and therefore superimpose the eigenfunction of the spatially most unstable varicose mode for the two-dimensional velocity profile computed from linear stability theory (see above). At the edges and outside of the nozzle ($|y| \geq L_1/2$) we smoothly ramp the superimposed eigenfunction to zero by multiplying it with

$$\theta(\eta) = exp\{-(1.2\eta)^8\} \quad . \qquad (3)$$

Here again η is equal to the $y-$coordinate normalized with the velocity half width $L_1/2$. We enforce an amplitude of the inflow disturbance so that $Q := max(\hat{u})/max(u) = 0.005$, where $\hat{}$ denotes the amplitude of the eigenfunction of the streamwise velocity variable u. The temporal frequency ω predicted by linear stability theory and confirmed by DNS is 2.7066. siniti

5. RESULTS

The simulation was started using an initially laminar rectangular jet profile throughout the entire computational domain on a coarse grid. After the initial transient the grid was refined to the actual grid using high order spline interpolation. Sampling was started after a second transient due to the interpolation had faded. A total of $1.2 \cdot 10^3$ samples from a dimensionless time interval of roughly 630 (270 periods of the harmonic excitation) using about $5 \cdot 10^4$ timesteps was analyzed. Note that because of the three-dimensionality of the flow no homogenous direction is present which could be used for additional averaging to improve statistical data. However, sector symmetry over the four quadrants of the rectangular profile can be exploited. In the following we first present instantaneous flow data to visualize the flow topology and secondly we show time- and sector-averaged data.

Instantaneous data

In figure 3 the instantaneous flow topology of the transition process is visualized by a density isosurface. We observe a strong growth of the linear instability mode in the laminar region. Rapidly three-dimensional disturbances of the initially two dimensional instability mode grow at the edges of the inflowing jet. A symmetrical vortex structure develops but breaks up almost immediately into small scale turbulence. To visualize this transitional vortical structure, in figure 4 we show a pressure isosurface enlarged in the transition region. Symmetrical vortices can be identified

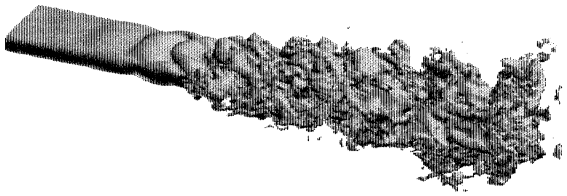

Figure 3: Snapshot of density isosurface.

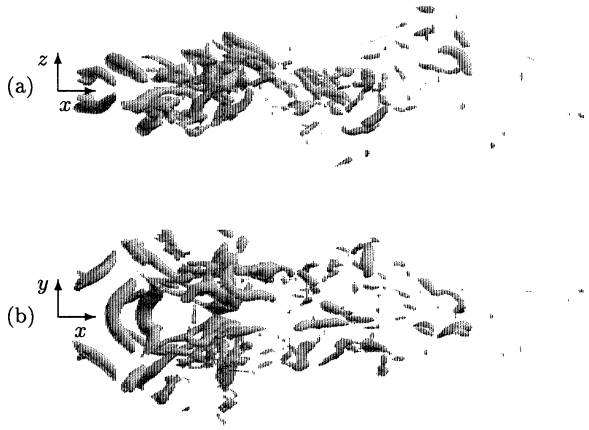

Figure 4: Snapshot of pressure isosurface in the transition region. Side view (a) and top view (b), flow from left to right.

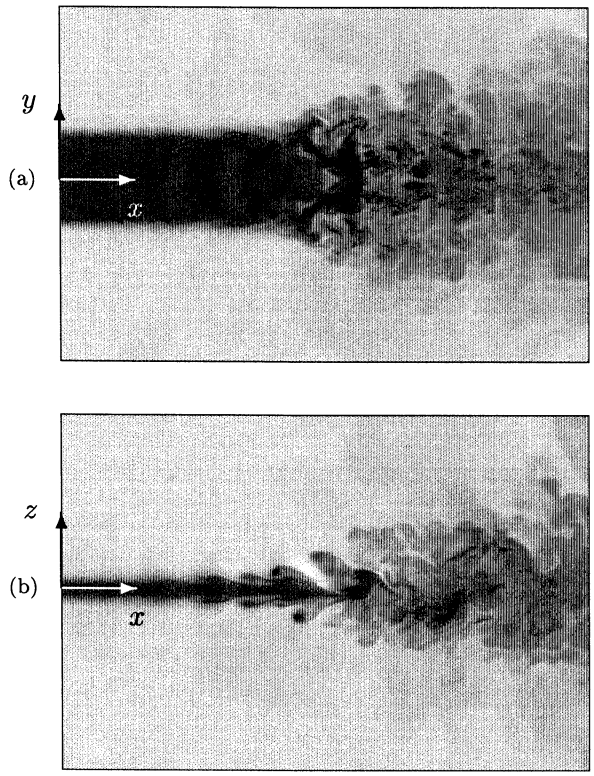

Figure 5: Snapshot of density contours along the major (a) and minor (b) axis of the jet at the same instant.

which deform and finally break up into disordered structures. Additionally, figure 5 depicts density plots in two cross-sections through the jet center. The excited varicose mode develops towards the antisymmetric sinuous mode and then transition rapidly leads to developed turbulence.

Statistically averaged data

To assess the mean properties of the analyzed flow we show sector- and time-averaged flow data at 9 equidistantly spaced downstream stations (each 35th grid plane which corresponds to a distance between the stations of $3.9L_2$) where the first station represents the inflow plane. We plot the data along the major and the minor axis of the jet. Note that the last station is still well before the beginning of the sponge zone at the end of the computational domain. We use the notation $<>$ for sector- and time averaged and $\tilde{}$ for Favre-averaged variables (the latter also includes sector averaging). In figure 6 the streamwise velocity profiles $<u>$ are shown. Ahead of the transition region the jet profile spreads only marginally due to diffusion. After transition has taken place, one observes a strong spreading of the profiles away from the major axis, so that the entire profile transforms towards an elliptical shape. In the transition region itself a non-monotonic profile is observed, which is caused by correlated large scale structures present in this region. It is known from experiments for non-axisymmetric jets (Tsuchiya *et al.*, 1986) that in the transition region a so called *saddle-back* profile occurs along the major axis of the mean flow. Here, the mean centerline streamwise velocity drops below the value reached in the surrounding shear layers. Our simulation is qualitatively in good agreement with these findings, see figure 6 (a), 5th and 6th profile.

In figure 7 the transverse velocity components $<v>$ and $<w>$ are plotted. The averaged velocity components in the direction orthogonal to the jet center planes vanish due to symmetry and are not shown. In the transition region one observes a peak of the cross-stream velocity components, which is roughly twice as high along the major axis as along the minor axis whereas in the turbulent regime the profiles flatten out again.

In order to deduce turbulent statistics we ex-

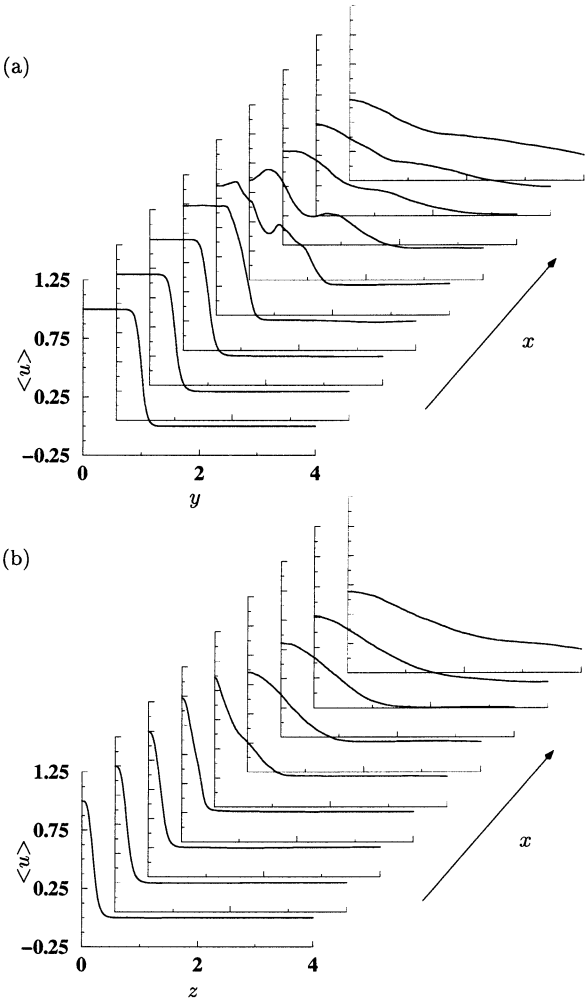

Figure 6: Mean streamwise velocity profiles at different downstream stations; along major (a) and minor (b) axis.

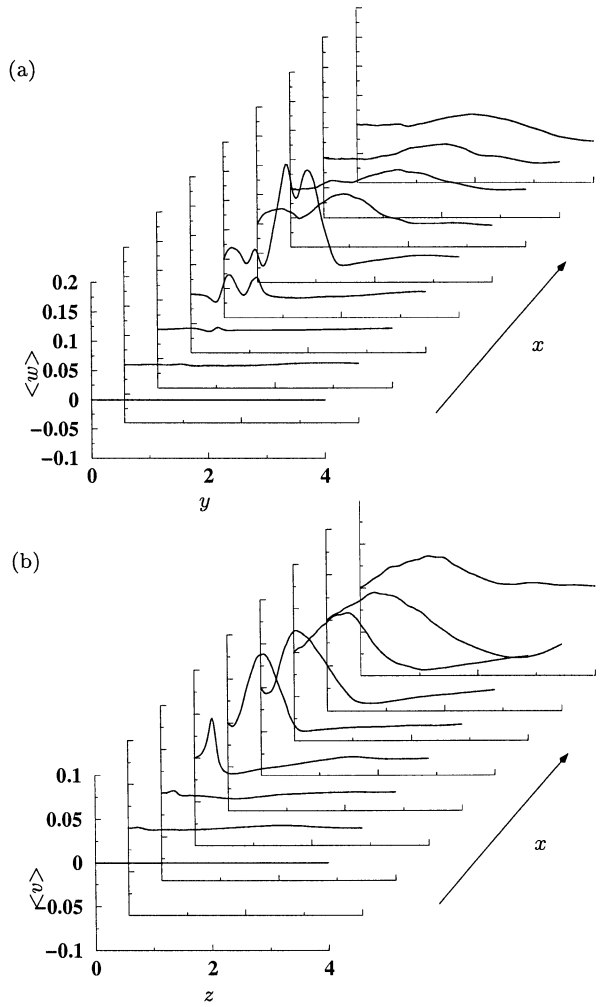

Figure 7: Mean cross-stream velocity profiles at different downstream stations; along major (a) and minor (b) axis.

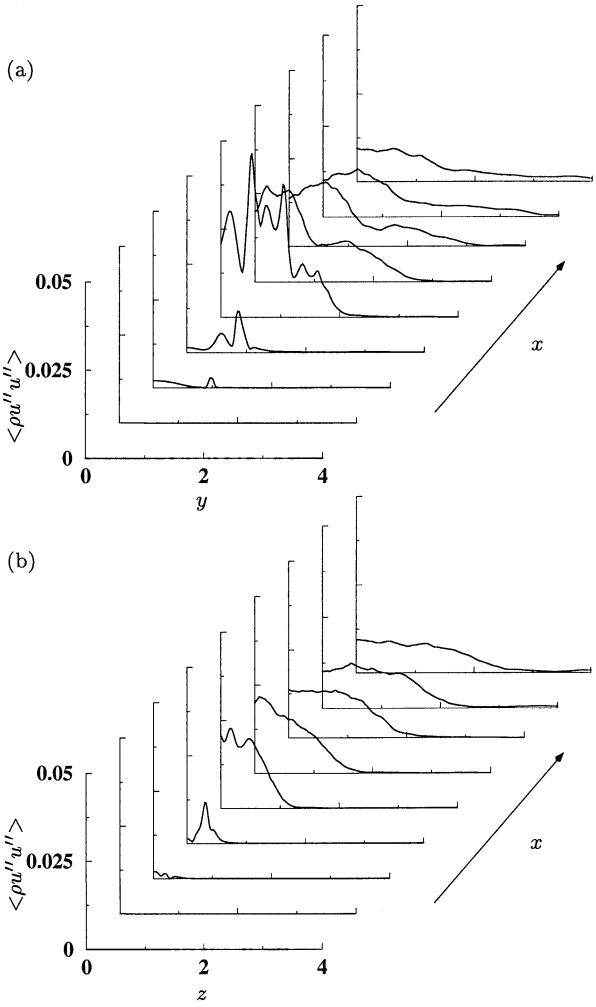

Figure 8: Reynolds normal stresses at different downstream stations; along major (a) and minor (b) axis.

amine the development of the turbulent kinetic energy k defined by $1/2 <\rho> \widetilde{u_k'' u_k''}$, the Reynolds normal stress $\tau_{11} =< \rho u'' u'' >$ and the Reynolds shear stresses $\tau_{12} =< \rho u'' v'' >$ and $\tau_{13} =< \rho u'' w'' >$. The number of samples computed is obviously not yet sufficient to get smooth profiles especially in the developed turbulent regime. The roughness of the profiles in the transition region, however, is believed to be caused by the deterministic inflow forcing used in this simulation. It is evident and also repeatedly shown in experiments, that the turbulence levels increase rapidly when the jet undergoes transition. However, this process probably depends strongly on parameters such as the shape of the nozzle, initial turbulence intensity, Reynolds number etc. This makes it difficult to compare computational and experimental data, since inflow conditions are usually not known with sufficient accuracy. In this simulation we find a rapid growth of the Reynolds stresses beginning roughly at a distance of $13L_2$ downstream of the nozzle, see figures 8 and 9. They reach peak values at the jet edges along the major axis, from where three-dimensional disturbances of the transition process originate. The same holds for the turbulent kinetic energy which is plotted in figure 10.

6. CONCLUDING REMARKS

We have presented first results of a Direct Numerical Simulation of a rectangular compressible jet configuration to investigate the transition process of non-axisymmetric jets and to provide reference data for Large-Eddy Simulation. We have imposed well defined inflow conditions in order to make validation of LES models possible. The transition process shows how the initially two-dimensional disturbances in the inflow region of the jet rapidly grow three-dimensional, which leads to a breakdown of the jet to small scale turbulence. Further analysis of the DNS data is in progress.

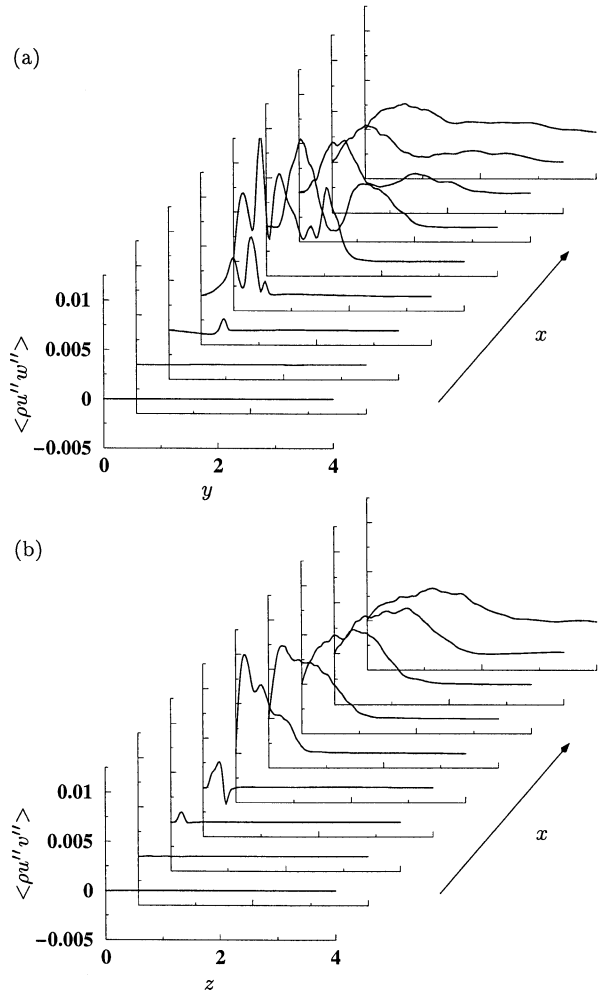

Figure 9: Reynolds shear stresses at different downstream stations; along major (a) and minor (b) axis.

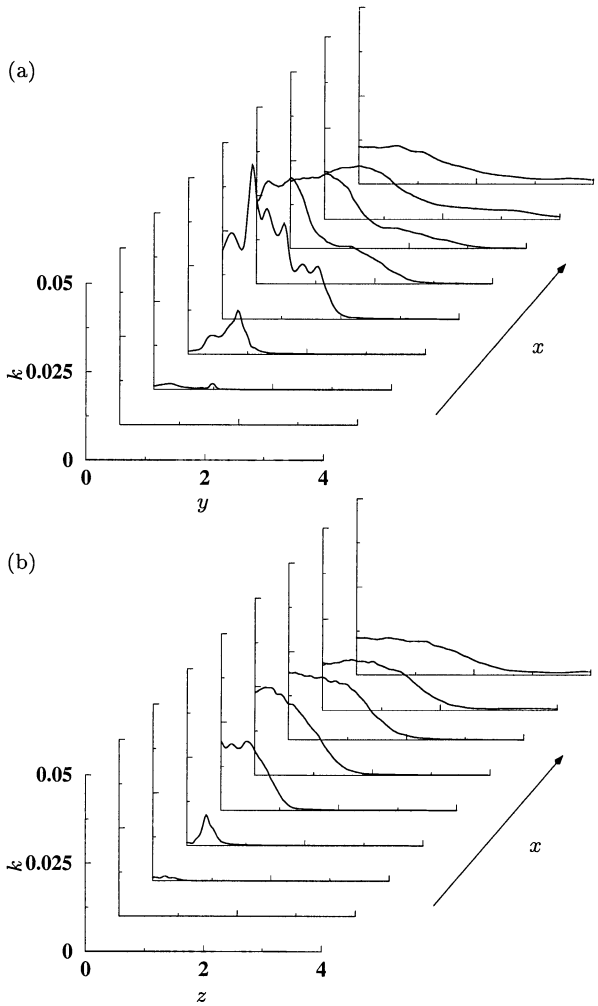

Figure 10: Turbulent kinetic energy k at different downstream stations; along major (a) and minor (b) axis.

REFERENCES

Adams, N. A., 1998. "Direct numerical simulation of turbulent compression corner flow." *Theor. Comp. Fluid Dyn.*, vol. 12, pp. 109–129.

Adams, N. A. and Shariff, K., 1996. "A high resolution hybrid compact-ENO scheme for shock-turbulence interaction problems." *J. Comput. Phys.*, vol. 127, pp. 27–51.

Gutmark, E. J. and Grinstein, F. F., 1999. "Flow control with noncircular jets." *Ann. Rev. Fluid Mech.*, vol. 31, pp. 239–72.

Lele, S. K., 1992. "Compact finite difference schemes with spectral-like resolution." *J. Comput. Phys.*, vol. 103, pp. 16–42.

Sforza, P. M. and Steiger, M. H., 1966. "Studies on three-dimensional viscous jets." *AIAA J.*, vol. 4(5), pp. 800–805.

Stanley, S. A. and Sarkar, S., 1999. "Direct numerical simulation of the developing region of turbulent planar jets." In *37th AIAA Aerospace Sciences Meeting and Exhibit*, AIAA 99-0288. AIAA, Reno, Nevada.

Thompson, K. W., 1987. "Time dependent boundary conditions for hyperbolic systems." *J. Comput. Phys.*, vol. 68(1), pp. 1–24.

Tsuchiya, Y., Horikoshi, C., and Sato, T., 1986. "On the spread of rectangular jets." *Exp. Fluids*, vol. 4, pp. 197–204.

Williamson, J. H., 1980. "Low-storage Runge-Kutta schemes." *J. Comput. Phys.*, vol. 35, pp. 48–56.

Yu, M.-H. and Monkewitz, P. A., 1990. "The effect on nonuniform density on the absolute instability of two-dimensional inertial jets and wakes." *Phys. Fluids*, vol. A2(7), pp. 1175–1181.